Study of muons in extensive air showers from ultra-high energy cosmic rays measured with the Telescope Array experiment

R. Takeishi[1,*] for the Telescope Array Collaboration

[1]Department of Physics, Sungkyunkwan University, Jang-an-gu, Suwon, Korea

Abstract. The origin of ultra-high energy cosmic rays (UHECRs) has been a long-standing mystery. One of the uncertainties in UHECR observation derives from the hadronic interaction model used for air shower Monte-Carlo (MC) simulations. The number of muons observed at ground level from UHECR induced air showers is expected to depend upon the composition of primary cosmic rays. The MC prediction also depends on hadronic interaction models. One may test the hadronic interaction models by comparing the measured number of muons with the MC prediction. The Telescope Array (TA) is the largest experiment in the northern hemisphere observing UHECR in Utah, USA. It aims to reveal the origin of UHECR by studying the energy spectrum, mass composition and anisotropy of cosmic rays by utilizing an array of surface detectors (SDs) and fluorescence detectors. We studied muon densities in the UHE extensive air showers by analyzing the signal of TA SD stations for highly inclined showers which should have high muon purity. A high muon purity condition is imposed that requires the geometry of the shower and relative position of the given station and implies that muons dominate the signal. On condition that the muons contribute about 65% of the total signal, the number of particles from air showers is typically $1.88 \pm 0.08(\mathrm{stat.}) \pm 0.42(\mathrm{syst.})$ times larger than the MC prediction with the QGSJET II-03 model for protons. The same feature was also obtained for other hadronic models, such as QGSJET II-04.

1 Introduction

The origin of ultra-high energy cosmic rays (UHECRs) has been a long-standing mystery of astrophysics. The Telescope Array (TA) experiment [1] located in Utah, USA is the largest experiment in the northern hemisphere observing UHECRs. It aims to reveal the origin of UHECRs by studying the energy spectrum, anisotropy and mass composition of cosmic rays. A UHECR entering the atmosphere interacts with atmospheric nuclei and generates the particle cascade, which is called an air shower. Observed signals of air shower particles and the air shower Monte Carlo (MC) simulation provide information of primary cosmic rays.

The energy range of UHECRs are beyond accelerator experiments, so UHECR air showers are not fully understood. The maximum target-frame energy of hadronic interactions accessible at accelerators at present is 10^{17} eV measured at the CERN LHC. The MC for cosmic rays in the energies above 10^{18} eV uses the extrapolated values of hadronic interaction parameters, such as cross section and multiplicity. The values of these parameters differ between hadronic interaction models, due to the uncertainty of modeling pion or kaon generation at the early stage of the air shower development. Thus inferences of UHECR composition from air shower measurements are model-dependent [2, 3], which is important to understand the origin of UHECRs since cosmic rays are deflected in the galactic and extragalactic magnetic fields.

Moreover, the Pierre Auger Observatory, which is located in Mendoza, Argentina, reported [4] a model-dependent deficit of muons in simulations of 30–80% relative to the data, 10^{19} eV. The Auger group also reported that the observed hadronic signal in UHECR air showers is 1.33 ± 0.16 (1.61 ± 0.21) times larger than the post-LHC MC prediction values for EPOS-LHC [5] (QGSJET II-04 [6]), including statistical and systematic errors [7].

The analysis of air shower components is important to obtain a realistic air shower model. The number of muons from a UHECR on the ground depends on the mass composition of primary cosmic rays. The MC prediction depends also on hadronic interaction models since it has information about the shower development at an early stage. One may test the hadronic interaction models by comparing the measured number of muons with the MC prediction. Furthermore, the lateral distribution of muons contains information about the hadronic interaction. In this work, we study the difference in the number of muons between experimental data and the MC. The difference as a function of lateral distance from the shower axis is also investigated. For that, we developed an analysis for muons from UHECR air showers with the TA surface detectors (SDs).

*e-mail: takeishi@skku.edu

2 Telescope Array experiment

The TA experiment measures air shower particles on the ground with the SDs and fluorescence light generated by the air shower with the fluorescence detectors (FDs). The TA SD array consists of 507 scintillation counters, located on a square grid with 1.2 km spacing, and covers 700 km^2 [8]. Each TA SD is composed of two layers of plastic scintillator with two photomultiplier tubes (PMTs), one for each layer. The detector has an area of 3 m^2 and each scintillator layer has 1.2 cm thickness. The scintillators and PMTs are contained in a stainless steel box which is mounted under a 1.2 mm thick iron roof to protect the detector from large temperature variations. The SD station is solar-powered and data are collected by a Wireless Local-Area Network (WLAN) system. The station measures air shower particles by collecting photons generated in scintillators through wavelength shifting fibers and detecting them with PMTs. The air shower events are triggered when at least three adjacent counters detect energy deposits equivalent to $\geq$ 3 minimum ionizing particles (MIPs) within 8 microseconds. The readout system then records SD signals equivalent to $\gtrsim$ 0.3 MIP detected within ±32 microseconds of the trigger time. The trigger efficiency is greater than 97% for primary particle energies above 10^{19} eV [8]. The calibration is performed every 10 minutes by monitoring histograms of signals from single atmospheric muons and comparing them with simulated distributions of energy deposition [8]. The correlation between the FADC values and the energy deposition is determined by the calibration.

The three TA FD stations are located around the SD array and view the sky above the array [9]. The stations consist of 38 telescopes with spherical mirrors. The fluorescence light from air showers is collected by the mirror and detected by PMTs. The trigger electronics select a track pattern of triggered PMTs in real time and record air shower tracks.

The TA SD event reconstruction consists of the following steps [10]: First, SD signals that are related to air shower events are selected by determining a cluster which is contiguous in space and time. Signals less than about 1.4 Vertical Equivalent Muon (VEM) are excluded from the cluster. This process reduces background signals from the random atmospheric muons, which occur uniformly in space and time at a rate of 0.05 per station within one event time period (±32 microseconds). Second, shower arrival time distributions of the SDs are fitted to determine the geometry of cosmic ray air showers. Third, a fit of the lateral distribution of charged particle densities at the SDs is performed using the lateral distribution function from the AGASA experiment [11, 12]. $S\,800$ is determined by the fit, which is the density of shower particles at a lateral distance of 800 m from the air shower axis. The energy of the cosmic ray is estimated by using a look-up table in $S\,800$ and the shower zenith angle. The table is obtained by a large statistics MC simulation using CORSIKA [13] and the QGSJET II-03 hadronic model [14]. Finally, the reconstructed energy is scaled to the energy measured by the TA FD, which is determined using calorimetric detection of an air shower energy deposition in the atmosphere [9, 15, 16] with less hadronic interaction dependence than the SD. The energy and angular resolutions for a primary energy within $10^{18.5}$ eV $< E < 10^{19.0}$ eV are 29% and 2.1°, respectively [17]. Those for energies above 10^{19} eV are 19% and 1.4°, respectively. The resolution of the distance from a shower axis is about 70-80 m within $10^{18.8}$ eV $< E < 10^{19.2}$ eV.

For the MC, we use CORSIKA v6.960, and QGSJET II-03 as a reference model for high energy hadronic interactions. The MCs for other models are also generated using the same MC procedure. We also use FLUKA2008.3c [18, 19] to model low energy hadronic interactions and EGS4 [20] to model electromagnetic interactions. The thinning [21] and "de-thinning" [22] techniques are used to reduce the computation time. The detector simulation is performed by using the Geant4 [23] toolkit.

The simulated cosmic ray energies range from $10^{16.55}$ to $10^{20.55}$ eV. The simulated zenith angle is isotropically distributed from 0° to 60°. The azimuth angle and core position are randomly distributed within the SD array. We applied the same reconstruction procedure as experimental data for the MC dataset.

3 Analysis

We use the TA SD 7 years' dataset recorded from 11 May 2008 through 11 May 2015, and the events reconstructed by the same method as the TA spectrum analysis [24] with an energy range $10^{18.8}$ eV $< E < 10^{19.2}$ eV. In this energy range, the mass composition of the primary cosmic rays is consistent with a light component within statistical and systematic errors as determined by $X_{\rm max}$ measurement using the TA FD [2, 3, 15, 25], where $X_{\rm max}$ is the depth in the atmosphere of air shower maximum. Thus we use the MC for proton primaries. We used the energy scale corrected by the FD (reconstructed energy scale) for the experimental data and the scale not corrected by the FD (thrown energy scale) for the MC. The experimental data are compared with the MC using the hadronic models QGSJET II-03, QGSJET II-04, Epos 1.99 [26] and Sibyll 2.1 [27].

The TA SD, made of plastic scintillators [8], is sensitive to the electromagnetic (EM) component (electrons and gammas) that are the predominant part of secondary particles from the air showers. The conversion rate of gammas to electrons in the TA SD is ∼20% at 1 GeV. To use the SD signals dominated by muons, we define the condition of the high *muon purity* using the MC. Then we compare the observed signal size from air shower particles with the MC prediction under the high muon purity condition.

The secondary particles generated in the atmosphere are attenuated by the interaction with atmospheric particles and they decay before reaching the ground. The EM components experience greater attenuation than muons over the same path length, because the EM components largely lose their energy by pair production and bremsstrahlung in the shower development but muons can penetrate the atmosphere down to the ground before decaying. Hence the ratio of the energy deposit of air shower

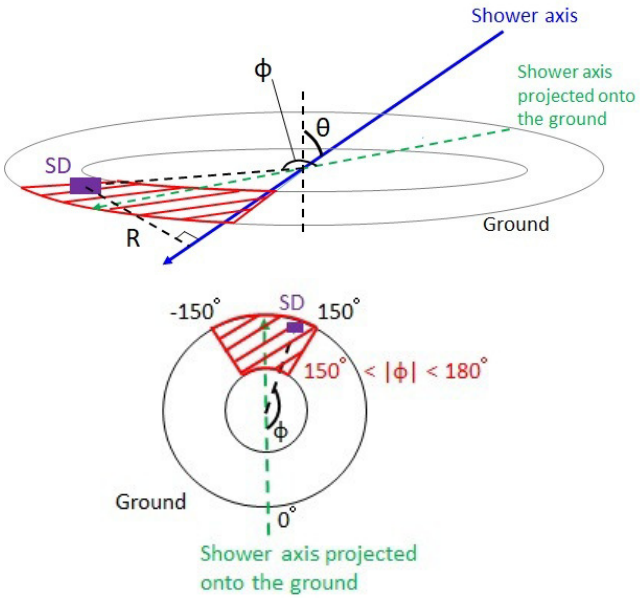

Figure 1. (top) Geometry definition of the muon analysis. An SD location on the ground is selected by ϕ and R to reduce the EM background. The muon purity in the SD signal is calculated in each (ϕ, R) bin. There are six bins for ϕ and 18 bins for R from 500 to 4500 m. The red shaded region in the figure shows the bin for $150^\circ < |\phi| < 180^\circ$ where the distance from the particle generation points on the shower axis is relatively larger than other ϕ bins, which is expected to be the least EM background bin. (bottom) Top view for the ϕ definition.

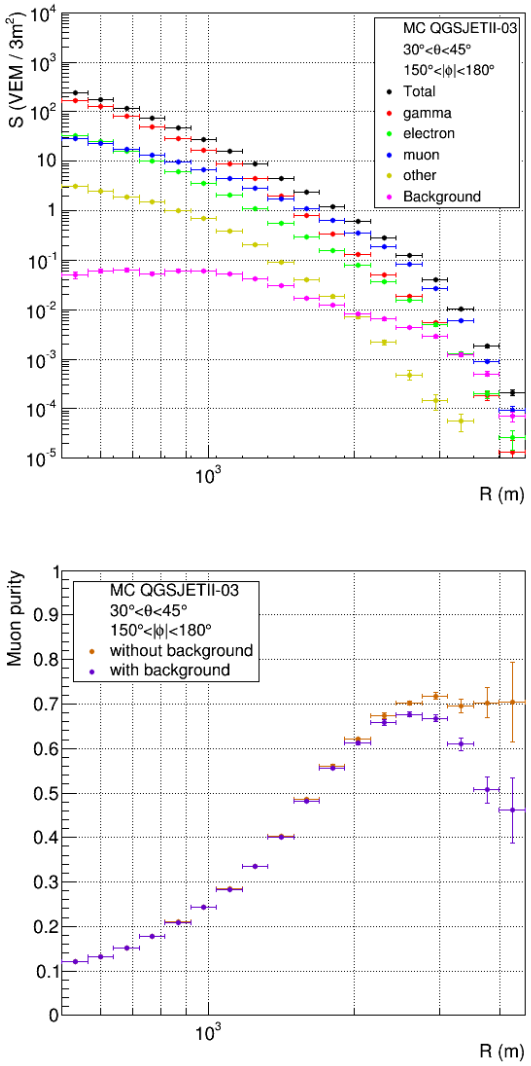

Figure 2. Lateral distributions of the air showers [29] (top) The air shower average signal of the MC with QGSJET Ⅱ-03 for $30^\circ < \theta < 45^\circ, 150^\circ < |\phi| < 180^\circ$, 500 m $< R <$ 4500 m. The red, green, blue, yellow, magenta and black represent gamma, electron, muon, other shower components, atmospheric muon background and the total of them, respectively. The vertical error bar shows the standard deviation. (bottom) The muon purity. The violet and orange show calculations with and without the atmospheric muon background, respectively.

muons to that of all particles, which consist of air shower and background components, in SD signals (hereafter this ratio is described as the muon purity) is expected to be larger for SDs more distant from secondary particle generation points on the shower axis. We classify the detector hits in the air shower events of the dataset using θ (the zenith angle), ϕ (the azimuth angle relative to the shower arrival direction projected onto the ground), and R (the distance from a shower axis). The geometry definition is described in Figure 1. When $\theta, |\phi|$ or R values become large, the path length of air shower particles increases, then the muon purity in SD signals is expected to be high.

The integrated FADC is calculated for each SD participating in the event. The FADC count, converted to VEM units, is entered in the histogram of the corresponding (θ, ϕ, R) bin. An SD which has no signal is assigned to the 0 VEM bin of the histogram. Figure 2 shows the lateral distributions of SD signals and the muon purity. The muon purity is mainly 60-70% on the high muon purity condition ($30^\circ < \theta < 45^\circ, 150^\circ < |\phi| < 180^\circ$, 2000 m $< R <$ 4000 m). We use these conditions to select high muon purity events for comparison of the data with the MC.

The statistical error of the average signal cannot be simply calculated for $R \gtrsim 1500$ m because the fraction of SDs with no hit signals is too large to determine lower and upper errors of the histogram. We assume the Poisson distribution $f(x) = N^x e^{-N}/x!$; N is the average value of the distribution and x is the variable for the signal size distribution. We calculated the average signal by the following equation: $n_0/n_{\rm all} = f(0) = e^{-N}$. Here n_0 and $n_{\rm all}$ are the entries of 0 VEM bin and the whole distribution, respectively. The probability that zero values appear n_0 times in $n_{\rm all}$ samples follows the binomial distribution, hence the standard deviation of n_0 is calculated as $\sqrt{n_{\rm all}\, p(1-p)}$, where p is $n_0/n_{\rm all}$.

4 Results

Figure 3 shows the lateral distributions of the signal and the ratio of the data to proton MC with various hadronic

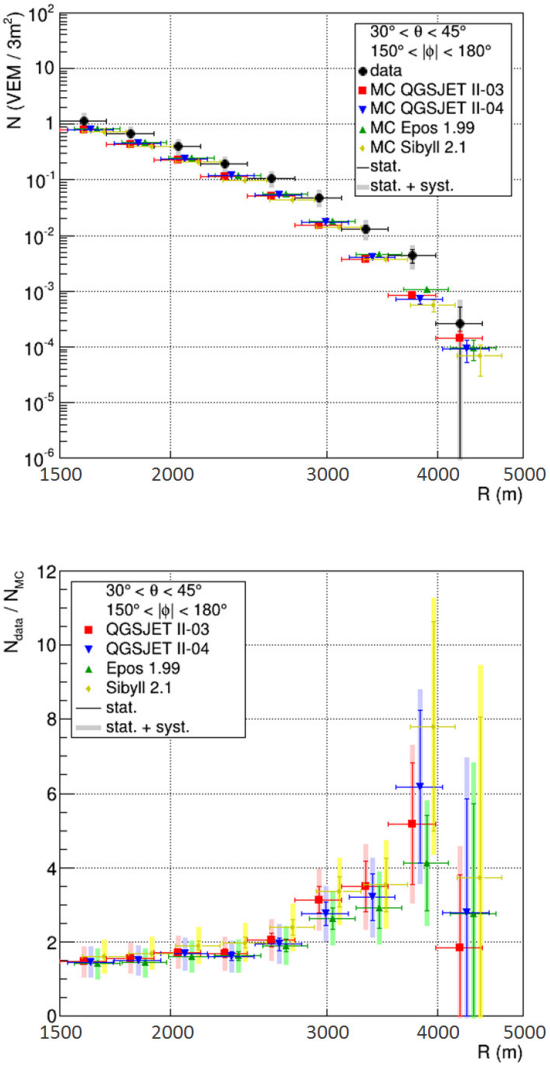

Figure 3. Lateral distributions of air showers of the data and the MCs for $30^\circ < \theta < 45^\circ, 150^\circ < |\phi| < 180^\circ$, 1500 m $< R <$ 4500 m [29]. (top) Lateral distributions of the average signal size assuming the histograms follow the Poisson distribution. The black, red, blue, green and yellow represent data, QGSJET II-03, QGSJET II-04, Epos 1.99 and Sibyll 2.1, respectively. To make error bars easy to see, the plots for the latter three models are shifted to the right. (bottom) The average ratio of the data to the MC.

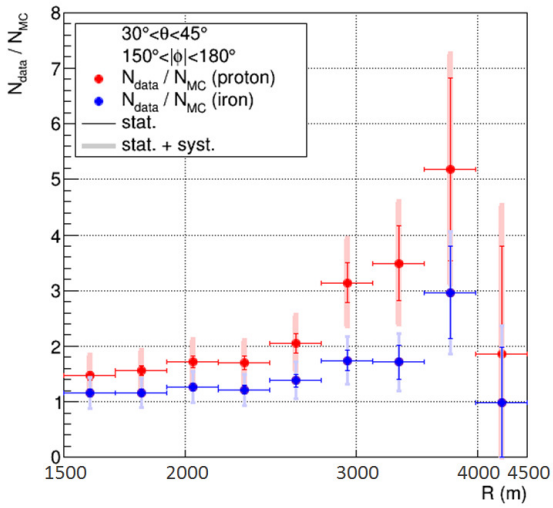

Figure 4. Ratios of the signal size of the data to the MCs for proton and iron [29]. The red and blue points respectively represent the ratios of the data to the MC for proton and that for iron. The vertical thin error bars and shaded thick error bars represent statistical errors and quadratic sums of statistical and systematic errors, respectively.

interaction models; QGSJET II-03, QGSJET II-04, Epos 1.99 and Sibyll 2.1. The ratios of the data to the MC with QGSJET II-03 are 1.72 ± 0.10(stat.) ± 0.37(syst.) at 1910 m $< R <$ 2160 m and 3.14±0.36(stat.)±0.69(syst.) at 2760 m $< R <$ 3120 m. The observed lateral distribution falls down slower than the MCs for all hadronic models used in the analysis. The data becomes closer to the MCs at $R \gtrsim$ 4000 m, since the atmospheric muon background dominates the SD signals at the distance.

We calculated lateral distributions of iron showers using the MC with QGSJET II-03. Figure 4 shows lateral distributions of the ratio of the data to the MCs for proton and iron. The average signal of the data is larger than the MC for iron for $R \gtrsim$ 2500 m. For the smaller distances, the difference between the data and the MC for iron is smaller than systematic errors.

Figure 5 shows the correlation between the muon purity expected from the MC and the ratio of the signal size of the data to that of the MC. On the high muon purity condition ($30^\circ < \theta < 45^\circ, 150^\circ < |\phi| < 180^\circ$, 2000 m $< R <$ 4000 m, magenta filled circle in Figure 5), the muon purity and the ratio of the data to the MC are 65% and 1.88 ± 0.08(stat.) ± 0.42(syst.), respectively. In the case of the low muon purity condition ($\theta < 30^\circ, |\phi| < 30^\circ$, 2000 m $< R <$ 4000 m, black open circle in Figure 5), they are 28% and 1.30 ± 0.06(stat.) ± 0.29(syst.), respectively. This figure shows larger differences in signal sizes between the data and the MC on higher muon purity conditions.

One of the systematic uncertainties of this work is caused by the uncertainty of the TA FD energy measurement, which is 21% [16]. An air shower model predicts that the number of particles from the EM and muonic components of the showers are proportional to $E^{1.03}$ and $E^{0.85}$ respectively, where E is the primary cosmic ray energy [28]. We assume the SD signal size is proportional to E and apply the systematic uncertainty of ±21% to the experimental data of signal sizes.

1 MIP signal size is determined by fitting a histogram of single atmospheric muons and searching for the peak position of the histogram. The systematic error from the accuracy of this calibration method is ±1.2% [29].

In the TA SD event reconstruction, we perform a cut on the SD signals not included in space-time clusters. This procedure reduces random atmospheric muon background in the dataset. We calculated the systematic error from this procedure as the difference in the ratio of signals with

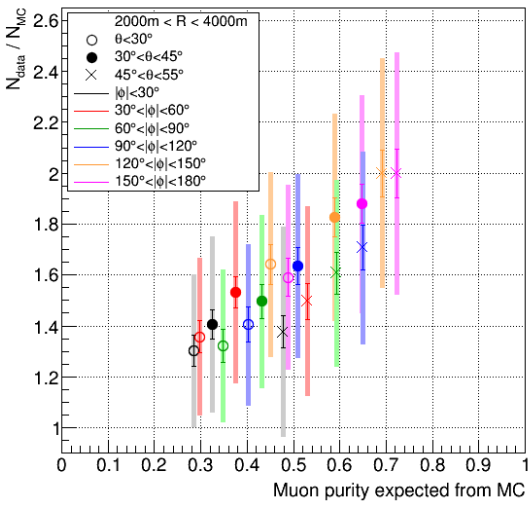

Figure 5. The correlation between the muon purity and the ratio of the signal size of the data to the MC with QGSJET II-03 for 2000 m $< R <$ 4000 m [29]. The black, red, green, blue, orange and magenta represent $|\phi| < 30°$, $30° < |\phi| < 60°$, $60° < |\phi| < 90°$, $90° < |\phi| < 120°$, $120° < |\phi| < 150°$ and $150° < |\phi| < 180°$, respectively. The open circle, filled circle and cross represent $\theta < 30°$, $30° < \theta < 45°$ and $45° < \theta < 55°$, respectively. The vertical thin error bars and shaded thick error bars represent statistical errors and quadratic sums of statistical and systematic errors, respectively.

cut to that without cut between the data and the MC. The calculated error is ±1%.

In this analysis, we calculated the average signal from air showers with an assumption of the signal size distribution following a Poisson distribution. We calculate the systematic error from this assumption by comparing the ratio of observed signals to the MC using the Poisson distribution, N, with that using the simple averaged value, S. The calculated values have R dependence and are within ±4%.

The TA SD reconstruction procedure conducts the fitting of lateral distributions without separating the SDs by the azimuth angle. The signal size of air showers in the shower arrival direction is larger than that in the shower forwarding direction compared to the same R. Thus the core position reconstructed by the procedure has a systematic shift on the side of the air shower arrival direction. We compared the signal size with reconstructed event parameters (E, θ, ϕ and core position) and that with input ones, using the MC. The bias of the signal size from the shift has R dependence and is in the range of 4-13%. We included them in the systematic error.

The average duty cycle of the SD array is approximately 95%, hence 5% of all the SDs in the dataset are possibly not working properly. The systematic uncertainty from this effect has R dependence and is within ±1% [29].

The total systematic uncertainty is $\pm(22-24\%)$ on the high muon purity condition ($30° < \theta < 45°, 150° < |\phi| < 180°$, 2000 m $< R <$ 4000 m). The error from the energy determination dominates in this analysis.

5 Conclusion

We developed an analysis for muons from UHE air showers with the TA scintillator SD. It uses θ, ϕ and R conditions to determine events with a high muon purity. The results imply that part of the discrepancy in signal sizes between the data and the MC is due to a muon excess in the data. The ratios of the signal size of the data to that of the MC with QGSJET II-03 are $1.72 \pm 0.10(\text{stat.}) \pm 0.37(\text{syst.})$ at 1910 m $< R <$ 2160 m and $3.14 \pm 0.36(\text{stat.}) \pm 0.69(\text{syst.})$ at 2760 m $< R <$ 3120 m on the high muon purity condition ($30° < \theta < 45°, 150° < |\phi| < 180°$, 2000 m $< R <$ 4000 m) at $10^{18.8}$ eV $< E < 10^{19.2}$ eV, The muon purity expected from the MC is about 65% on that condition. The measurement presented here is qualitatively consistent with the result of the Auger experiment [4, 7], where the threshold energy of air shower particles (~10 MeV for TA SD and 300 MeV for Auger SD) and R conditions are different. We also found that the lateral distribution of the data falls down slower than the MC on the high muon purity condition, resulting in a larger ratio of the data to the MC at larger R values. This result provides information to improve reliability of hadronic interaction models.

Acknowledgments

The Telescope Array experiment is supported by the Japan Society for the Promotion of Science (JSPS) through Grants-in-Aid for Priority Area 431, for Specially Promoted Research JP21000002, for Scientific Research (S) JP19104006, for Specially Promoted Research JP15H05693, for Scientific Research (S) JP15H05741 and for Young Scientists (A) JPH26707011; by the joint research program of the Institute for Cosmic Ray Research (ICRR), The University of Tokyo; by the U.S. National Science Foundation awards PHY-0601915, PHY-1404495, PHY-1404502, and PHY-1607727; by the National Research Foundation of Korea (2017K1A4A3015188; 2016R1A2B4014967; 2017R1A2A1A05071429, 2016R1A5A1013277); by the Russian Academy of Sciences, RFBR grant 16-02-00962a (INR), IISN project No. 4.4502.13, and Belgian Science Policy under IUAP VII/37 (ULB). The foundations of Dr. Ezekiel R. and Edna Wattis Dumke, Willard L. Eccles, and George S. and Dolores Doré Eccles all helped with generous donations. The State of Utah supported the project through its Economic Development Board, and the University of Utah through the Office of the Vice President for Research. The experimental site became available through the cooperation of the Utah School and Institutional Trust Lands Administration (SITLA), U.S. Bureau of Land Management (BLM), and the U.S. Air Force. We appreciate the assistance of the State of Utah and Fillmore offices of the BLM in crafting the Plan of Development for the site. Patrick Shea assisted the collaboration with valuable advice on a variety of topics. The people and the

officials of Millard County, Utah have been a source of steadfast and warm support for our work which we greatly appreciate. We are indebted to the Millard County Road Department for their efforts to maintain and clear the roads which get us to our sites. We gratefully acknowledge the contribution from the technical staffs of our home institutions. An allocation of computer time from the Center for High Performance Computing at the University of Utah is gratefully acknowledged.

References

[1] M. Fukushima, Prog. Theor. Phys. Suppl. **151**, 206 (2003).
[2] T. Stroman *et al.*, Proc. 34th ICRC, 361 (2015).
[3] T. Fujii *et al.*, Proc. 34th ICRC, 320 (2015).
[4] A. Aab *et al.* (Pierre Auger Collaboration), Phys. Rev. D **91**, 032003 (2015); Erratum, Phys. Rev. D **91**, 059901 (2015).
[5] K. Werner, F. M. Liu, and T. Pierog, Phys. Rev. C **74**, 044902 (2006).
[6] S. Ostapchenko, Phys. Rev. D **83**, 014018 (2011).
[7] A. Aab *et al.* (Pierre Auger Collaboration), Phys. Rev. Lett. **117**, 192001 (2016).
[8] T. Abu-zayyad *et al.*, Nucl. Instrum. Methods. A **689**, 87 (2012).
[9] R. U. Abbasi *et al.*, Astropart. Phys. **80**, 131 (2016).
[10] D. Ivanov, Ph.D. thesis, Rutgers-The State University of New Jersey, Department of Physics and Astronomy, Piscataway, New Jersey, USA (2012).
[11] M. Takeda *et al.*, Phys. Rev. Lett. **81**, 1163 (1998).
[12] M. Takeda *et al.*, Astropart. Phys. **19**, 447 (2003).
[13] D. Heck *et al.*, Forschungszentrum Karlsruhe Report FZKA, 6019 (1998).
[14] S. Ostapchenko, Nucl. Phys. B, Proc. Suppl. **151**, 147 (2006).
[15] R. U. Abbasi *et al.*, ApJ **858**, 76 (2018).
[16] T. Abu-Zayyad *et al.*, Astropart. Phys. **61**, 93 (2015).
[17] R. U. Abbasi *et al.*, Astropart. Phys. **86**, 21 (2017).
[18] A. Ferrari *et al.*, Tech. Rep. 2005-010, CERN (2005).
[19] G. Battistoni *et al.*, AIP Conf. Proc. **896**, 31 (2007).
[20] W. R. Nerson *et al.*, Tech. Rep. 0265 SLAC (1985).
[21] M. Kobal *et al.*, Astropart.Phys. **15**, 259 (2001).
[22] B. T. Stokes *et al.*, Astropart.Phys. **35**, 759 (2012).
[23] J. Allison *et al.*, IEEE Trans. Nucl. Sci. **53**, 270 (2006).
[24] T. Abu-Zayyad *et al.*, ApJ **768**, L1 (2013).
[25] R.U. Abbasi *et al.*, Astropart. Phys. **64**, 49 (2015).
[26] T. Pierog and K. Werner, Nucl. Phys. Proc. Suppl. **196**, 102 (2009).
[27] E. J. Ahn *et al.*, Phys. Rev. D **80**, 094003 (2009).
[28] J. Matthews, Astropart. Phys. **22**, 387 (2005).
[29] R. U. Abbasi *et al.* (Telescope Array Collaboration), Phys. Rev. D **98**, 022002 (2018).